Supporting Information

Direct Observation of Strand Passage by DNA-Topoisomerase and Its Limited Processivity

Katsunori Yogo, Taisaku Ogawa, Masahito Hayashi, Yoshie Harada, Takayuki Nishizaka, and Kazuhiko Kinosita Jr.

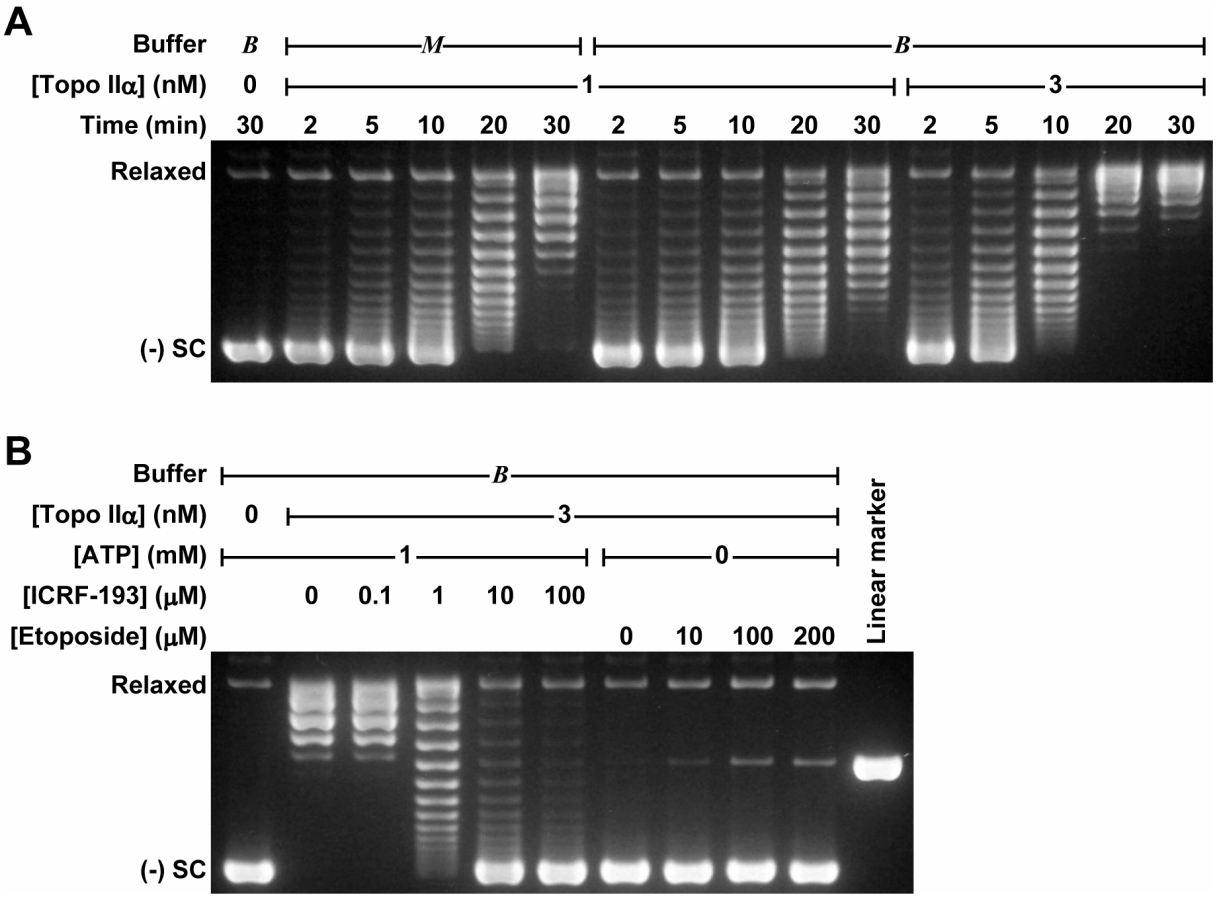

Figure S1. Bulk supercoil relaxation activity of topo IIα. The enzyme at the indicated concentration was incubated with 5 nM pBR322 plasmid (negatively supercoiled) and 1 mM ATP (unless indicated otherwise) for the indicated time at 37°C in 20 μL of buffer B for bulk assay or buffer M for microscopy. Buffer B was the base buffer described in the main text (10 mM Tris pH 7.9, 100 mM NaCl, 50 mM KCl, 5mM $MgCl_2$, 0.1 mM EDTA) containing, in addition, 0.1 mg/mL BSA. For buffer M, the base buffer was supplemented with 5 mM DTT, 0.1 mg/mL dimethylated casein, 0.2 % Tween-20, and 800,000-fold dilution of SYBR Gold. The reaction was started by the addition of 1 μL of the enzyme diluted in buffer B containing 0.5 mM DTT, and terminated by the addition of 2 μL of 5% SDS and 100 mM EDTA. Samples were mixed with 2 μL of gel loading buffer (50% glycerol, 0.9% SDS, 0.05% Bromophenol Blue), heated at 70°C for 2 min, subjected to electrophoresis in a 1% agarose gel in 90 mM Tris-borate pH 8.4 and 2 mM EDTA, and stained with 10,000-fold dilution of SYBR Gold. (**A**) Time courses of relaxation. (–)SC, negatively supercoiled plasmid; relaxed, relaxed circular plasmid. (**B**) Effects of topoisomerase-specific drugs. ICRF-193, a bis(2,6-didioxopiperazine) derivative, is a potent inhibitor of type II topoisomerase with 50% inhibition at ~2 μM [16]. Epotoside inhibits religation of DNA, producing double-strand breaks irrespective of the presence of ATP [17]. Assays were made as in **A** for the reaction period of 30 min. Samples with epotoside were incubated, prior to electrophoresis, with 200 μg/mL proteinase K at 45°C for 30 min to digest topo IIα. Linear DNA marker was generated by digesting pBR322 by EcoRI. The yield of linearized DNA at 200 μM epotoside is below 10% at the enzyme/pBR322 molar ratio of four under similar conditions [17].

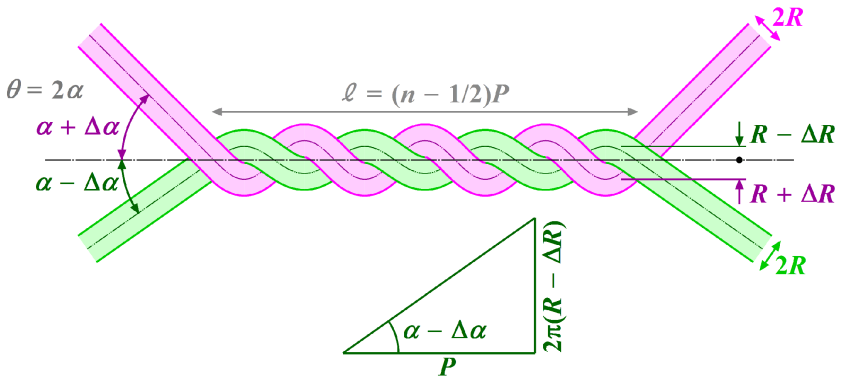

Figure S2. A geometrical model for a DNA braid. The model has been described by Charvin et al. [7] for the case of a symmetric braid ($\Delta\alpha = 0$). Here, the angles between the DNA and braid axis are $\alpha+\Delta\alpha$ (magenta) and $\alpha-\Delta\alpha$ (green), which are assumed to be maintained through the braid. In the braid, the distances between the DNA axis and braid axis are taken as $R+\Delta R$ (magenta) and $R-\Delta R$ (green). The pitch P is then given as $P = 2\pi(R + \Delta R)/\tan(\alpha + \Delta\alpha)$ for magenta DNA and $P = 2\pi(R - \Delta R)/\tan(\alpha - \Delta\alpha)$ for green DNA. The two pitches must be the same in a braid, leading to $P = 2\pi R\cot\alpha(1 - \Delta\alpha^2/\cos\alpha^2)$ where terms higher than $\Delta\alpha^2$ have been neglected. For a braid of $(n - 1/2)$ turns (made by winding one DNA around the other for n turns as described in the main text), its length ℓ is given by $\ell = (n - 1/2)P$. The effect of the asymmetry ($\Delta\alpha$) is of the second order and is practically negligible, and thus $\ell \sim 2\pi(n - 1/2)R\cot\alpha = 2\pi(n - 1/2)R\tan(\pi/2 - \theta/2)$, where $\theta = 2\alpha$ is the angle between the two DNAs. This final result is the same as that by Charvin et al. [7], and the only merit of the calculation above is to show that asymmetry does not matter as long as $\Delta\alpha << 1$ (radian). Note that the geometrical model would fail at $\alpha > 45°$ where the magenta and green rods would overlap partially, although R here represents an entropic radius of DNA [22] which is much larger than the geometrical radius of ~1 nm and thus the failure would not be a sudden one expected for solid ropes.

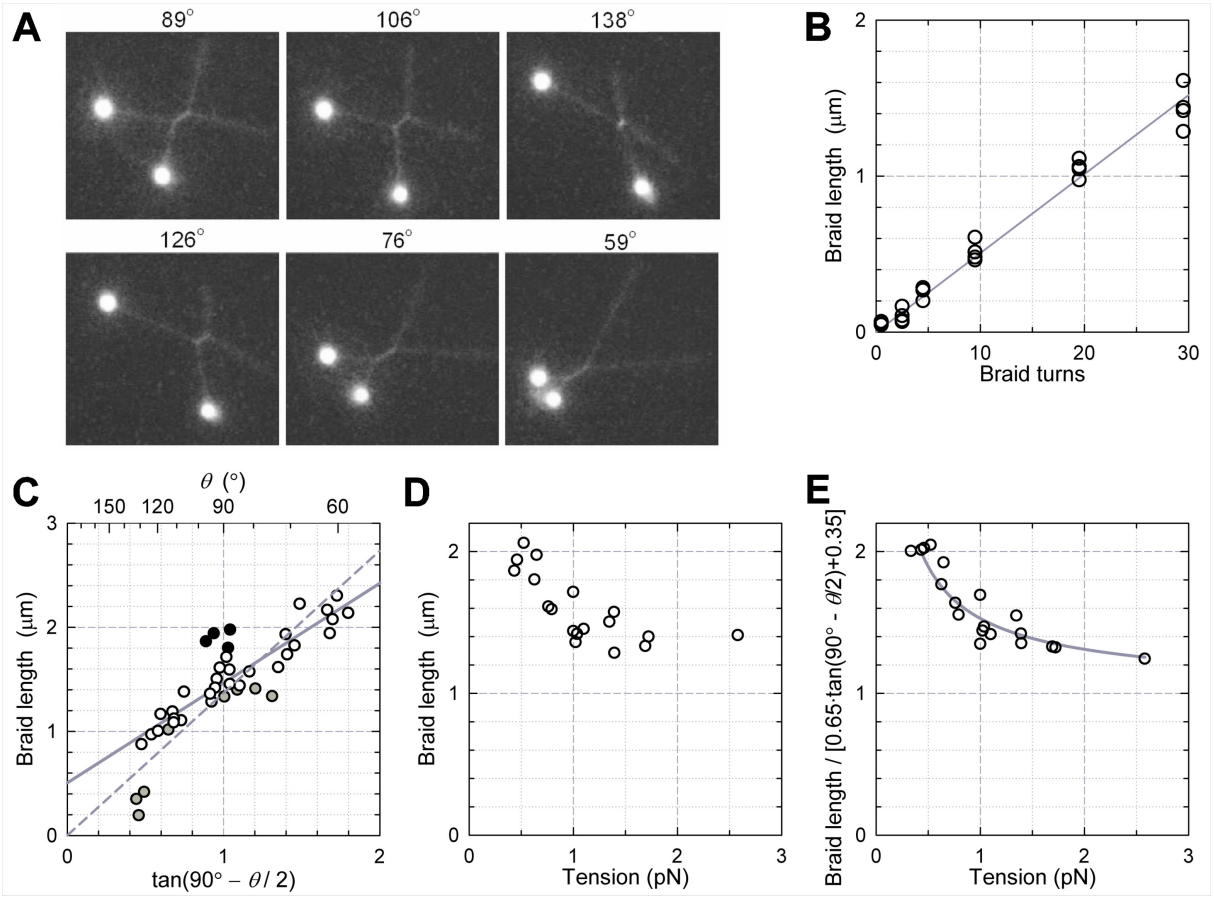

Figure S3. Determinants of braid length. Pairs of DNA were braided and the braid lengths estimated from fluorescence images as described in the main text, except that topoisomerase was not included in the medium. (**A**) Fluorescence images of a DNA braid of n = 30, showing dependence of the braid length on braid angles. (**B**) Proportionality between braid length and braid turns (n – 1/2) for θ around 90° (range 75°-95°). (**C**) Angle dependence of the braid length for n = 30. The lower horizontal axis is chosen to test the geometrical model in Figure S2. Open circles, tension between 0.7 and 1.4 pN; black circles, below 0.7 pN; gray circles, above 1.4 pN. Dashed line shows regression passing through the origin (geometrical model) for open circles, with $\ell = 1.37\tan(90° - \theta/2)$ where ℓ is the braid length in μm. A better fit is obtained if we allow the line to deviate from the origin (solid line), with $\ell = 0.51 + 0.96\tan(90° - \theta/2)$. Deviation from the geometrical model (Figure S2) is expected for $\theta > 90°$, and the observed braid pitch of ~50 nm (ℓ/n), close to the persistence length of DNA, also suggests that bending the DNA may cost additional energy. (**D**) Tension dependence of the braid length (n = 30) for θ around 90° (range 79°-97°). (**E**) Braid lengths in **D** converted to those at $\theta = 90°$ by assuming the angle dependence shown in the solid line in **C**. Solid curve shows fit assuming that the normalized braid length depends on the tension F as $F^{-3/4}$ [7]: $\ell = 0.90 + 0.63F^{-3/4}$ where F is in pN. In the main text and in Figure S4 below, we estimate the braid turns n from the observed braid length ℓ and tension F assuming this tension dependence and the solid line in **C**: $\ell = [(n - 1/2)/(29.5\cdot1.47)][0.51 + 0.96\tan(90° - \theta/2)][0.90 + 0.63F^{-3/4}]$ or $n = 1/2 + 72\ell$ / {[0.53 + tan(90° - θ/2)](1.43 + $F^{-3/4}$)}. The root-mean-square deviation of the 58 measured braid lengths from this phenomenological equation (four data with tan(90° - θ/2) < 0.5 excluded) is 0.12 μm, which is a measure of the reliability of the length estimates.

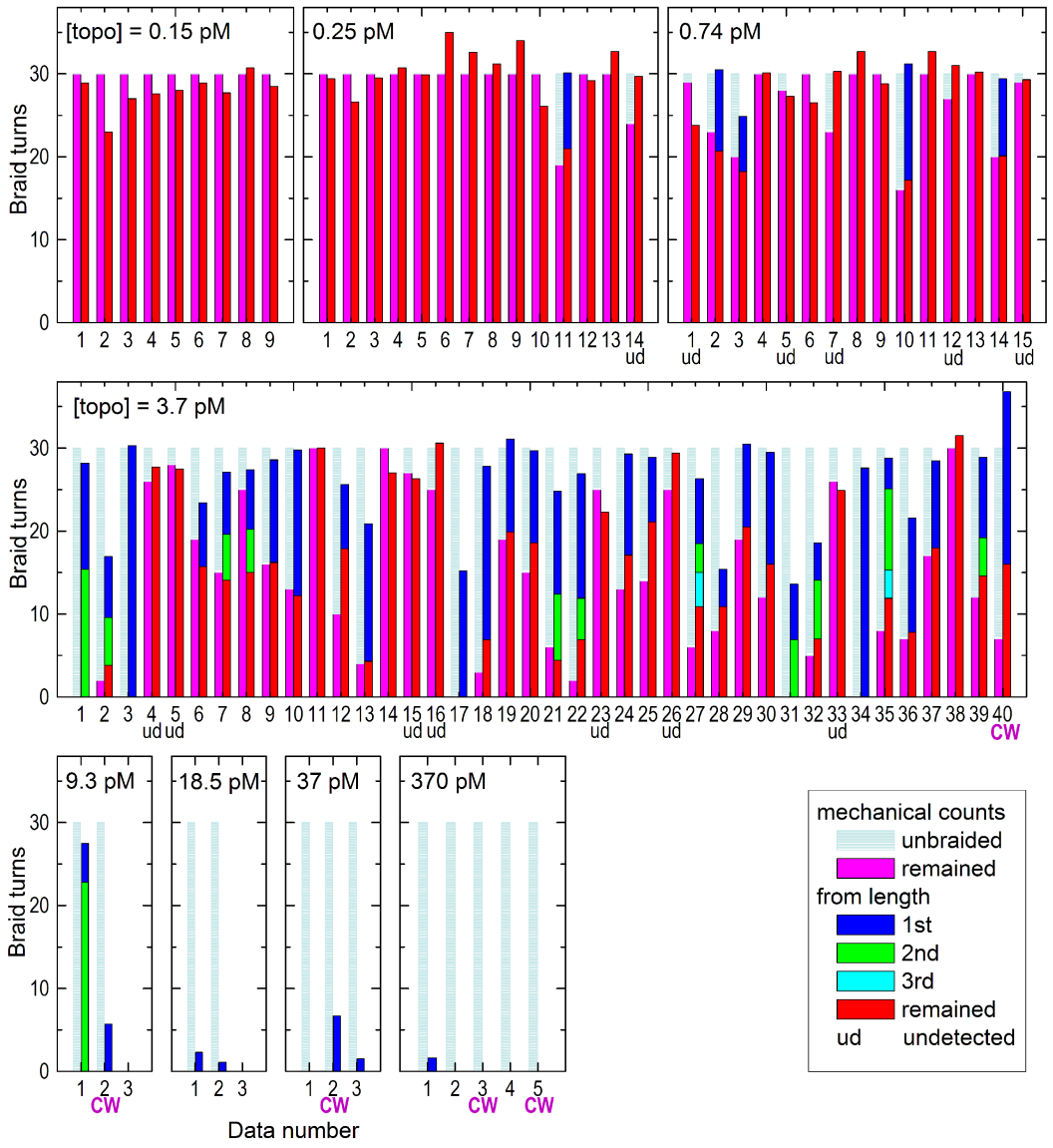

Figure S4. Summary of individual unbraiding reactions. Results from each experiment are shown in paired bars, the left bar showing the braid turns counted by mechanical winding/unwinding and the right bar showing the observed braid lengths which have been converted to the braid turns by the last equation in Figure S3. All the left bars are given the same height of 30 turns, the count in the initial mechanical winding. Note that the count at time 0 may have been smaller, due to premature unbraiding particularly at high [topo IIα]s. The magenta portions show the braid turns that remained at 300 s, estimated by mechanical unbraiding. Some of these may be underestimated, due to unbraiding by topo IIα during the process of mechanical unbraiding. The height of the bars on the right corresponds to the braid length at time 0. The height deviates from 30, because the determination of the braid length and the conversion to braid turns both involve errors, and because premature unbraiding took place at high [topo IIα]s. For the same reasons, the magenta portion in the left bar and the red portion in the right bar do not match precisely. "ud" indicates the cases where the mechanical count suggested unbraiding but a decrease in the braid length could not be detected reliably. Note that failure in detecting a length change can be inferred only when the initial length was apparently preserved; when unbraiding is detected both in the mechanical counts and length changes, there is always a possibility that an additional short unbraiding event(s) has taken place without being detected. CW, clockwise braid.

Text S1. DNA fluctuations in a braid.

Here we present an order-of-magnitude estimation of the extent of DNA fluctuations in a braid. The treatment below is not rigorous nor precise, and numerical values should be regarded as such. The braids we consider are those in our experiments, where the four ends of a braid are pulled at nearly right angles under ~1 pN of tension.

First we consider longitudinal fluctuations of the middle of a 16-μm DNA held at its two ends. For DNA as a worm-like chain, the relation between its extension L and applied tension F can be approximated [23] by $FA/k_BT = (1/4)[(1 - L/L_0)^{-2} - 1] + L/L_0$, where L_0 is the contour length, A (~50 nm) the persistence length, and k_BT (~4.1 pN·nm at room temperature) the thermal energy ($L/L_0 \sim 0.85$ for $F = 1$ pN). When the two ends of a 16-μm DNA are fixed, its middle is constrained by two halves of the DNA each with a spring constant [24] $K_{//} = \partial F/\partial L$, which, for L_0=8 μm and $F = 1$ pN in our experiment, is calculated as 1.5×10^{-3} pN/nm. The middle thus fluctuate, in the direction along the length of DNA, with an amplitude Δz characterized by $\langle\Delta z^2\rangle = k_BT/2K_{//} \sim (37\text{ nm})^2$.

In a DNA braid, the two DNA molecules are constrained laterally, but fluctuations of each DNA along the braid axis is not much restricted by the other DNA unless the tension is high enough to force the two DNAs physically touch with each other (R ~ 1 nm in Figure S2). Thus, the average amplitude of fluctuation of one DNA in a braid, along the braid length, will also be $\sim\langle\Delta z^2\rangle^{1/2}$ or ~37 nm. Fluctuations beyond this value are not rare: the probability of fluctuations beyond $\pm2\langle\Delta z^2\rangle^{1/2} \sim \pm74$ nm is ~5% and beyond $\pm3\langle\Delta z^2\rangle^{1/2} \sim \pm110$ nm is still as high as ~0.3%. The frequency of such fluctuations can very roughly be estimated as follows. The diffusion coefficient D of a 1-μm DNA segment is of the order of $k_BT/6\pi\eta a \sim 5\times10^{-13}$ m^2/s where $\eta \sim 0.9\times10^{-3}$ Ns/m^2 is the viscosity of water and a = 0.5 μm (the dependence on the size, a, is modest and thus we take the length arbitrarily as 1 μm and adopt the simplest formula for D, for a sphere of radius a, which is an underestimate for the thin DNA segment). Free diffusion of the DNA segment over 74 nm thus takes $(74\text{ nm})^2/2D \sim 0.005$ s. When restricted by the rest of DNA as springs, diffusion over 74 nm = $2\langle\Delta z^2\rangle^{1/2}$ succeeds in ~5% of the cases, or once in ~0.1 s. Similarly, diffusion of the middle of DNA over 110 nm would take place once in ~4 s. Note that these frequency values are underestimated.

Thus, in the case of a simple DNA cross (a half-turn braid), topoisomerase does not have to bind precisely at the apex: even if it binds ±0.1 μm away, the binding site will fluctuate to the apex (or the other DNA will fluctuate to the binding site) more often than once a second. The effective target size for topo IIα binding is of the order of 0.2 μm in our experiments. In a long braid, a topo IIα molecule will continue to unbraid it until the topo IIα gets out of the braid zone by ~0.1 μm, as long as the topo IIα stays on the binding site on one DNA and remains active.

Next we consider lateral fluctuations of DNA. Suppose that a DNA of extension L is fixed at its two ends such that its tension is F. When its middle is displaced laterally by Δx, the two halves of DNA pull the middle back each with a force $F\cdot[\Delta x/(L/2)]$, or each with a spring constant [24] $K_\perp = F/(L/2)$. Mean square displacement of the middle is given by $\langle\Delta x^2\rangle = k_BT/2K_\perp$. The pitch of our braid is ~50 nm (~1.5 μm / 30 turns; Figure S3), which is a measure of L above for lateral fluctuations. For L = 50 nm and F = 1 pN, $\langle\Delta x^2\rangle^{1/2} \sim 7$ nm. The two DNAs in our braid are separated laterally by an average distance of this magnitude (R in Figure S2). For lateral fluctuations of this size, DNA may be considered to consists of segments of length A (persistence length) that move relatively independently, with a diffusion coefficient an order of magnitude larger than the above D of 5×10^{-13} m^2/s. Lateral encounters of two DNAs in a braid should thus be frequent, well above a thousand times a second (depending on how an encounter is defined).

Video S1. Unbraiding of a 30(29.5)-turn DNA braid in two bursts.
The movie consists of three portions (initial setup, first unbraiding burst, second burst resulting in complete unbraiding) as indicated by green horizontal bars in Figure 1C in the main text, with 1-s blackouts in between. The time displayed on the lower right matches that in Figure 1C. The white bar that appears at time 0 indicates 1.8 μm, the initial braid length. Note that the stage, and thus the DNA roots, were slightly moved to the right between ~70 and ~75 s to increase the tension (Figure 1D). The movie taken at 30 frames/s has been running-averaged for 30 frames, and the intensity adjusted to highlight DNA (bead images are saturated).

References

1. Liu LF, Liu CC, Alberts BM (1979) T4 DNA topoisomerase: a new ATP-dependent enzyme essential for initiation of T4 bacteriophage DNA replication. Nature 281: 456-461.
2. Brown PO, Cozzarelli NR (1979) A sign inversion mechanism for enzymatic supercoiling of DNA. Science 206: 1081–1083.
3. Mizuuchi K, Fisher LM, O'Dea MH, Gellert M (1980) DNA gyrase action involves the introduction of transient double-strand breaks into DNA. Proc Natl Acad Sci USA 77: 1847-1851.
4. Wang JC (1998) Moving one DNA double helix through another by a type II DNA topoisomerase: the story of a simple molecular machine. Q Rev Biophys 31: 107-144.
5. Schoeffler AJ, Berger JM (2008) DNA topoisomerases: harnessing and constraining energy to govern chromosome topology. Q Rev Biophys 41: 41-101.
6. Strick TR, Croquette V, Bensimon D (2000) Single-molecule analysis of DNA uncoiling by a type II topoisomerase. Nature 404: 901-904.
7. Charvin G, Bensimon D, Croquette V (2003) Single-molecule study of DNA unlinking by eukaryotic and prokaryotic type-II topoisomerases. Proc Natl Acad Sci USA 100: 9820–9825.
8. Stone MD, Bryant Z, Crisona NJ, Smith SB, Vologodskii A, et al. (2003) Chirality sensing by *Escherichia coli* topoisomerase IV and the mechanism of type II topoisomerases. Proc Natl Acad Sci USA 100: 8654-8659.
9. Nöllmann M, Stone MD, Bryant Z, Gore J, Crisona NJ, et al. (2007) Multiple modes of *Escherichia coli* DNA gyrase activity revealed by force and torque. Nat Struct Mol Biol 14: 264-271.
10. Renodon-Cornière A, Jensen LH, Nitiss JL, Jensen PB, Sehested M (2002) Interaction of human DNA topoisomerase II α with DNA: Quantification by surface plasmon resonance. Biochemistry 41: 13395-13402.
11. Mueller-Planitz F, Herschlag D (2008) Coupling between ATP binding and DNA cleavage by DNA Topoisomerase II: A unifying kinetic and structural mechanism. J Biol Chem 283: 17463-17476.
12. Smiley RD, Collins TRL, Hammes GG, Hsieh TS (2007) Single-molecule measurements of the opening and closing of the DNA gate by eukaryotic topoisomerase II. Proc Natl Acad Sci USA 104: 4840-4845.
13. Zechiedrich EL, Osheroff N (1990) Eukaryotic topoisomerases recognize nucleic acid topology by preferentially interacting with DNA crossovers. EMBO J 9: 4555-4562.
14. Koster DA, Wiggins CH, Dekker NH (2006) Multiple events on single molecules: Unbiased estimation in single-molecule biophysics. Proc Natl Acad Sci USA 103: 1750-1755.
15. McClendon AK, Rodriguez AC, Osheroff N (2005) Human topoisomerase IIα rapidly

relaxes positively supercoiled DNA. Implications for enzyme action ahead of replication forks. J Biol Chem 280: 39337-39345.
16. Tanabe K, Ikegami Y, Ishida R, Andoh T (1991) Inhibition of topoisomerase II by antitumor agents bis(2,6-dioxopiperazine) derivatives. Cancer Res 51: 4903-4908.
17. Bromberg KD, Burgin AB, Osheroff N (2003) A two-drug model for etoposide action against human topoisomerase IIα. J Biol Chem 278: 7406-7412.
18. Harada Y, Ohara O, Takatsuki A, Itoh H, Shimamoto N, et al. (2001) Direct observation of DNA rotation during transcription by *Escherichia coli* RNA polymerase. Nature 409: 113-115.
19. Hayashi M, Harada Y (2007) Direct observation of the reversible unwinding of a single DNA molecule caused by the intercalation of ethidium bromide. Nucleic Acids Res 35: e125.
20. Arai Y, Yasuda R, Akashi K, Harada Y, Miyata H, et al.(1999) Tying a molecular knot with optical tweezers. Nature 399: 446-448.
21. Yasuda R, Noji H, Yoshida M, Kinosita KJr, Itoh H (2001) Resolution of distinct rotational substeps by submillisecond kinetic analysis of F_1-ATPase. Nature 410: 898-904.
22. Marko JF (1997) Supercoiled and braided DNA under tension. Phys. Rev. E 55: 1758-1772.
23. Βυσταμαντε Χ, Μαρκο ϑΦ, Σιγγια ΕΔ, Σμιτη ΣΒ (1994) Εντροπιχ ελαστιχιτψ οϕ λ-phage DNA. Science 265: 1599-1600.
24. Strick TR, Allemand J-F, Bensimon D, Croquette V (1998) Behavior of supercolied DNA. Biophys. J. 74: 2016-2028.